DESIGN OF A DYNAMIC POSITIONING SYSTEM USING MODEL-BASED CONTROL

By:

Dr. Asgeir J. Sørensen, ABB Industri AS, Marine Division

Dr. Svein I. Sagatun, ABB Industri AS, Marine Division

Professor Thor I. Fossen, Norwegian University of Science and Technology, Dept. of Engineering Cybernetics

Presented at IFAC Workshop on Control Applications in Marine Systems (CAMS'95), Trondheim, Norway, May 1995.

Published in the IFAC Journal *Control Engineering Practice*, Volume **4**, No. **3**, 1996.

DESIGN OF A DYNAMIC POSITIONING SYSTEM USING MODEL-BASED CONTROL

Asgeir J. Sørensen*, Svein I. Sagatun and Thor I. Fossen*****

**ABB Industri AS, Hasleveien 50, P. O. Box 6540 Rodeløkka, N-0501 Oslo, NORWAY*
(E-mail: asgeir.sorensen@noina.abb.telemax.no)
***ABB Industri AS, Hasleveien 50, P. O. Box 6540 Rodeløkka, N-0501 Oslo, NORWAY*
(E-mail: sis@ttsint.no)
****The Norwegian Institute of Technology, Department of Engineering Cybernetics, N-7034 Trondheim, NORWAY (E-mail: tif@itk.unit.no)*

Abstract. A dynamic positioning (DP) system includes different control functions for the automatic positioning and guidance of marine vessels by means of thruster and propeller actions. This paper describes the control functions which provide station-keeping and tracking. The DP controller is a model-based control design, where a new modified LQG feedback controller and a model reference feedforward controller are applied. A reference model calculates appropriate reference trajectories. Since it is not desirable, nor even possible, to counteract the wave-frequency movement caused by first-order wave loads, the control action of the propulsion system should be produced by the low-frequency part of the vessel movement caused by current, wind and second-order mean and slowly varying wave loads. A Kalman-filter-based state estimator and a Luenberger observer are used to compute the low-frequency feedback and feedforward control signals. Full-scale experiments with a multipurpose supply ship demonstrate the performance of the proposed controller.

Key Words. Dynamic positioning, model-based control, hydrodynamics, sea trials, marine systems.

1. INTRODUCTION

Dynamic positioning (DP) systems have been commercially available for marine vessels since the 1960s. The first DP systems were designed by using conventional PID controllers in cascade with low-pass and/or notch filters. From the middle of the 1970s more advanced control techniques based on optimal control and Kalman filter theory were proposed by Balchen et al. (1976). This work has later been modified and extended by Balchen et al. (1980a, b), Grimble *et al.* (1980a, b), Fung and Grimble (1983) and Sælid *et al.* (1983).

In this paper a model-based control scheme which provides both station-keeping and tracking (also denoted as marked position) of ships is proposed. This algorithm is an extension of the modified LQG control algorithm proposed by Balchen (1993). A reference model is introduced in order to compute appropriate reference trajectories. Since it is not desirable to counteract the wave-frequency (WF) movement caused by first-order wave loads, the control action of the propulsion system is produced by the low-frequency (LF) part of the vessel movement caused by current, wind and second-order mean and slowly varying wave loads. A Kalman-filter-based state estimator and a Luenberger observer are used to compute the feedback and feedforward control signals.

2. MATHEMATICAL MODELLING

In order to achieve good performance of the control system it is necessary to derive a sufficiently detailed mathematical model of the vessel and thruster system. The model parameters are

identified by running an off-line parallel extended Kalman filter algorithm, see (Fossen *et al.* ,1995).

2.1 Kinematics

The different reference frames used in dynamic positioning are illustrated in Fig. 1 and described below.

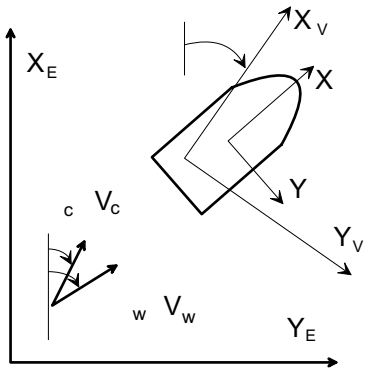

Fig. 1. Reference frames.

- The **earth-fixed** reference frame is denoted as the $X_E Y_E Z_E$-frame.
- The **vessel-parallel** frame, denoted as the $X_V Y_V Z_V$-frame, is fixed in the earth-fixed frame and rotated to the desired heading angle ψ_o and then translated to the desired x_o and y_o position coordinates.
- The **body-fixed** frame, denoted as the XYZ-frame, is fixed to the vessel body with the origin located at the centre of gravity.

The linear velocity of the ship in the body-fixed frame relative to the earth-fixed frame is given by the transformation:

$$\dot{\eta} = J(\eta)\upsilon \qquad (1)$$

where the earth-fixed vessel position and heading, and the body-fixed surge, sway and yaw velocities are defined by the vectors $\eta = [x, \ y, \ \psi]^T$ and $\nu = [u, \ v, \ r]^T$. The rotation matrix $J(\eta)$ is:

$$J(\eta) = \begin{bmatrix} \cos\psi & -\sin\psi & 0 \\ \sin\psi & \cos\psi & 0 \\ 0 & 0 & 1 \end{bmatrix} . \qquad (2)$$

2.2 Vessel Dynamics

The mathematical model describing the vessel dynamics is separated into a LF model and a WF model. The WF motions are assumed to be caused by first-order wave loads. Assuming small amplitudes these motions can be represented by a linear model.

The LF motions are assumed to be caused by second-order mean and slowly varying wave loads, current loads, wind loads and thrust forces. These motions are generally nonlinear, but linear approximations around certain operating points can be found. In the DP literature there has been some confusion related to the classification of energy dissipation in the WF and LF models. Mostly, linear damping is omitted in the derived LF models. In this paper linear damping proportional to the vessel velocities in surge, sway and yaw is introduced in both the LF model and the WF model. In addition, nonlinear eddy-making damping proportional to the square of the velocity is included in the LF model. It is important to notice that for decreasing velocities, linear damping becomes more significant than nonlinear damping.

An important contribution to linear damping in the LF model is viscous laminar skin friction and wave drift damping, which must not be mixed with the frequency-dependent wave radiation damping used in the WF model (Faltinsen, 1990). The effect of wave radiation damping is negligible in the LF model due to the low frequency of oscillation. Wave drift damping can be interpreted as added resistance for a ship advancing in waves and is, according to Faltinsen and Sortland (1987), the most important damping contribution to the surge motion in higher sea states. The wave drift damping is proportional to the square of the significant wave height. There is also wave drift damping in sway and yaw. However, relative to the eddy-making damping the importance of the wave drift damping is small for the sway and yaw motion. Linear skin friction may also be important for surge, especially for low sea states when the boundary layer is laminar, but cannot be completely neglected in sway and yaw. For higher sea states the viscous skin friction becomes turbulent and hence nonlinear (Faltinsen *et al*., 1986). The eddy-making damping is most important for sway and yaw motions. The cross-flow principle and strip theory are used to calculate viscous damping in sway and yaw, while direct pressure integration is used to calculate eddy-making damping in surge. Both methods are semi-empirical in the sense that empirical drag coefficients are employed. Instead of applying semi-empirical methods, model tests are often used.

2.2.1 Nonlinear Low-Frequency Model

The nonlinear body-fixed coupled equations of the LF motion in surge, sway and yaw are written:

$$M\dot{\upsilon} + C_{RB}(\upsilon)\upsilon + C_A(\upsilon_r)\upsilon_r + D_L\upsilon + D_{NL}(\upsilon_r, \gamma_r)\upsilon_r = \tau_{wind} + \tau_{wave2} + \tau \ . \qquad (3)$$

Here, τ is a control vector consisting of forces and moment in surge, sway and yaw provided by the thruster system. The effect of current is included in the relative velocity vector according to $\upsilon_r = \left[u - u_c, \quad v - v_c, \quad r\right]^T$. The components of the current are defined as:

$$\begin{aligned} u_c &= V_c \cos\left(\beta_c - \psi\right) \\ v_c &= V_c \sin\left(\beta_c - \psi\right) \end{aligned} \tag{4}$$

where V_c and β_c are the current velocity and direction respectively, see Fig. 1. Notice that current velocity in yaw is not considered. The mass matrix M including added mass is defined as:

$$M = \begin{bmatrix} m - X_{\dot{u}} & 0 & 0 \\ 0 & m - Y_{\dot{v}} & -Y_{\dot{r}} \\ 0 & -N_{\dot{v}} & I_z - N_{\dot{r}} \end{bmatrix} \tag{5}$$

where m is the vessel mass, and I_z is the moment of inertia about the z-axis. The zero-frequency added mass in surge, sway and yaw due to accelerations along the corresponding axes are defined as $X_{\dot{u}} < 0$, $Y_{\dot{v}} < 0$, and $N_{\dot{r}} < 0$. Assuming small vessel velocity and starboard and port symmetries, the added mass in sway due to the angular acceleration in yaw is equal to the added mass in yaw due to the sway acceleration, that is $Y_{\dot{r}} = N_{\dot{v}}$. Hence, the mass matrix is symmetrical and positive definite.

The skew-symmetric Coriolis and centripetal matrix of the rigid body can be formulated:

$$C_{RB}(\upsilon) = \begin{bmatrix} 0 & 0 & -mv \\ 0 & 0 & mu \\ mv & -mu & 0 \end{bmatrix}. \tag{6}$$

The effect of current may be divided into two parts according to Wichers (1993); the potential part and the viscous part. The potential part of the current is here modelled in a skew-symmetric Coriolis matrix, that is:

$$C_A(\upsilon_r) = \begin{bmatrix} 0 & 0 & Y_{\dot{v}} v_r + Y_{\dot{r}} r \\ 0 & 0 & -X_{\dot{u}} u_r \\ -Y_{\dot{v}} v_r - Y_{\dot{r}} r & X_{\dot{u}} u_r & 0 \end{bmatrix}. \tag{7}$$

The motivations for the skew-symmetric formulation of Coriolis terms are to achieve a compact notation and to demonstrate stability in certain applications (Fossen, 1994). The strictly positive damping matrix $D_L > 0$, caused by linear wave drift damping and laminar skin friction damping is defined as:

$$D_L = \begin{bmatrix} -X_u & 0 & 0 \\ 0 & -Y_v & -Y_r \\ 0 & -N_v & -N_r \end{bmatrix}. \tag{8}$$

The nonlinear damping vector can be formulated:

$$D_{NL}(\upsilon_r, \gamma_r)\upsilon_r = \begin{bmatrix} 0.5\,\rho_w L_{pp} D C_{cx}(\gamma_r)\,|u_r|u_r \\ 0.5\,\rho_w L_{pp} D C_{cy}(\gamma_r)\,|v_r|v_r \\ 0.5\,\rho_w L_{pp}^2 D C_{c\psi}(\gamma_r)\,|v_r|v_r \end{bmatrix} \tag{9}$$

where ρ_w is the density of water, L_{pp} is the length between the ship perpendiculars, D is the draft and $C_{cx}(\gamma_r)$, $C_{cy}(\gamma_r)$ and $C_{c\psi}(\gamma_r)$ are the non-dimensional drag coefficients in surge, sway and yaw respectively. The drag coefficients can be found by model testing. The relative drag angle is found from the following relation:

$$\gamma_r = \text{atan2}\left(v_{r,} u_r\right). \tag{10}$$

The effect of wind may be divided into mean, slowly-varying and rapidly-varying wind loads. The components of the wind velocities are defined according to:

$$\begin{aligned} u_w &= V_w \cos\left(\beta_w - \psi\right) \\ v_w &= V_w \sin\left(\beta_w - \psi\right) \end{aligned} \tag{11}$$

where V_w and β_w are the wind velocity and direction respectively, see Fig. 1. The wind velocity is assumed to be much larger than the vessel velocity, such that the wind load vector in surge, sway and yaw are formulated:

$$\tau_{wind} = \begin{bmatrix} 0.5\,\rho_a A_{wx} C_{wx}(\gamma_w)\,|u_w|u_w \\ 0.5\,\rho_a A_{wy} C_{wy}(\gamma_w)\,|v_w|v_w \\ 0.5\,\rho_a A_{wy} L_{oa} C_{w\psi}(\gamma_w)\,|v_w|v_w \end{bmatrix} \tag{12}$$

where ρ_a is the density of air, L_{oa} is the overall length of the vessel, and A_{wx} and A_{wy} are the lateral and longitudinal areas of the non-submerged part of the ship projected on the xz-plane and yz-plane. $C_{wx}(\gamma_w)$, $C_{wy}(\gamma_w)$ and $C_{w\psi}(\gamma_w)$ are the non-dimensional wind coefficients in surge, sway and yaw respectively. These coefficients are often found by model testing or by employing semi-empirical formulas as presented in (Isherwood, 1972). The relative wind angle is defined as:

$$\gamma_w = \beta_w - \psi \ . \tag{13}$$

The wave drift loads contribute to a significant part of the total excitation force in the LF model. The second-order wave effects are divided into mean and slowly varying wave loads. The determination of the second-order wave effects can be done by means of quadratic transfer functions (Faltinsen, 1990). However, this is time-consuming and requires a large amount of input data. An approximate approach proposed by Newman (1974), using frequency dependent wave drift coefficients may be applied. By dividing the sea wave spectrum (usually of Pierson-Moskowitz type) into N equal frequency intervals with corresponding wave frequency ω_j and amplitude A_j , the wave drift loads for surge (i = 1), sway (i = 2) and yaw (i = 3) are found to be:

$$\tau^i_{wave2} = \bar{\tau}^i_{wm} + \tau^i_{wsv} = 2\left(\sum_{j=1}^{N} A_j \left(T^i_{jj}\left(\omega_j, \beta_{wave} - \psi\right)\right)^{\frac{1}{2}} \cos\left(\omega_j t + \varepsilon_j\right)\right)^2 \tag{14}$$

where $T^i_{jj}\left(\omega_j\right) > 0$ is the frequency-dependent wave drift function, β_{wave} is the mean wave direction, and ε_j is a random phase angle. A disadvantage with the approximation (14) is the numerical generation of high-frequency components of no physical meaning. By modifying (14) this can be avoided. (14) can also be extended to include wave spreading. In general, the second-order wave loads are much less than the first-order wave loads. The second-order wave loads are proportional to the square of the wave amplitude, whereas the first-order wave loads are proportional to the wave amplitude. This means that the second-order wave loads have an increased importance for increasing sea states, at least up to a certain sea state.

2.2.2 Linear Low-Frequency Model

For the purpose of controller design, it is convenient to apply a linear LF model around zero relative vessel velocity. In order to reduce the coupling in the rotation matrix, the vessel position and heading angle are referred to the vessel-parallel frame. Assuming small yaw rotations about the desired heading angle $\Delta\psi=\psi-\psi_o$, the rotation matrix (2) can be approximated by the identity matrix. The measured position and heading signals must be transformed to the vessel-parallel frame before they are processed by the estimator and the controller. The linear LF state-space model can be formulated as:

$$\begin{aligned} \dot{x}_L &= A_L x_L + B_L \tau + \Gamma_L w_L \\ y_L &= C_L x_L + v \ . \end{aligned} \tag{15}$$

The state-space vector is defined as $x_L = \left[\upsilon^T, \ \eta^T\right]^T$, where for notation simplicity the incremental symbol Δ is omitted. w_L is a 3-dimensional disturbance vector consisting of current, wind and wave drift loads. y_L is a 3-dimensional measurement vector containing the surge and sway positions, and the yaw angle. v is a 3-dimensional vector of sensor noise which is assumed to be Gaussian white noise. The 6×6 system matrix is then written:

$$A_L = \begin{bmatrix} -M^{-1}D_L & 0_{3\times3} \\ I_{3\times3} & 0_{3\times3} \end{bmatrix} \tag{16}$$

where $I_{3\times3}$ is the 3×3 identity matrix and $0_{3\times3}$ is the 3×3 zero matrix. The 6×3 control input matrix is independent of the actual thruster configuration and becomes:

$$B_L = \begin{bmatrix} M^{-1} \\ 0_{3\times3} \end{bmatrix}. \tag{17}$$

The 6×3 disturbance input matrix is:

$$\Gamma_L = \begin{bmatrix} M^{-1} \\ 0_{3\times3} \end{bmatrix}. \tag{18}$$

Converting the position and heading measurements to the vessel-parallel frame, the 3×6 LF measurement matrix becomes:

$$C_L = \begin{bmatrix} 0_{3\times3} & I_{3\times3} \end{bmatrix}. \tag{19}$$

2.2.3 Linear Wave-Frequency Model

Since it is possible to obtain results in irregular seas by linearly superposing results from regular wave components, it is sufficient to analyse the vessel in regular sinusoidal waves of small steepness. The hydrodynamic problem in regular waves is solved as two sub-problems which are added together to give the total linear wave induced loads (Faltinsen, 1990):

- **Wave Reaction:** Forces and moments on the vessel when the vessel is forced to oscillate with the wave excitation frequency. The hydrodynamic loads are identified as added mass and wave radiation damping terms.
- **Wave Excitation:** Forces and moments on the vessel when the vessel is restrained from

oscillating and there are incident waves. This gives the wave excitation loads which are composed of so-called Froude-Kriloff and diffraction forces and moments.

The coupled equations of WF motion in surge, sway and yaw are assumed to be linear, and can in the vessel-parallel frame be formulated as:

$$M(\omega)\ddot{\eta}_W + D_p(\omega)\dot{\eta}_W = \tau_{wave1} \qquad (20)$$

where the WF motion vector for surge and sway translations and yaw rotations is defined as $\eta_W = [\eta_1, \ \eta_2, \ \eta_6]^T$. τ_{wave1} is a 3-dimensional excitation vector which will be modified for varying vessel heading relative to the incident wave direction. M(ω) is a 3×3 mass matrix containing frequency dependent added mass coefficients in addition to the vessel mass and moment of inertia. $D_p(\omega)$ is a 3×3 wave radiation damping matrix. An important feature of the added mass terms and the wave radiation (potential) damping terms are the memory effects or the frequency dependence. This can be taken into account by introducing a convolution integral or a so-called retardation function (Newman, 1977). The structure of the mass and damping matrices are the same as in (5) and (8).

The WF response spectra of the surge and sway translations and the yaw rotations can be found in irregular seas by reformulating (20) as a transfer function matrix and by representing the wave loads by wave load spectra. These response spectra are often approximated in controller design by synthetic white-noise-driven processes consisting of three uncoupled harmonic oscillators with damping (Sælid *et al.*, 1983). In state-space form a synthetic WF model can be written:

$$\begin{aligned} \dot{x}_W &= A_W x_W + \Gamma_W n \\ y_W &= C_W x_W \end{aligned} \qquad (21)$$

where the state-space vector is defined as $x_W = [\eta_W^T, \ \xi^T]^T$. y_w is a 3-dimensional measurement vector of the WF surge and sway positions, and the WF yaw angle. The 6×6 system matrix is derived to be:

$$A_W = \begin{bmatrix} A_W^{11} & A_W^{21} \\ I_{3\times3} & 0_{3\times3} \end{bmatrix} \qquad (22)$$

where

$$A_W^{11} = \begin{bmatrix} -2\zeta_1\omega_1 & 0 & 0 \\ 0 & -2\zeta_2\omega_2 & 0 \\ 0 & 0 & -2\zeta_6\omega_6 \end{bmatrix}$$

$$A_W^{21} = \begin{bmatrix} -\omega_1^2 & 0 & 0 \\ 0 & -\omega_2^2 & 0 \\ 0 & 0 & -\omega_6^2 \end{bmatrix}$$

where ζ_i is the relative damping ratio, and ω_i is the natural frequency. The relative damping ratio ζ_i is often in the range of 0.05-0.2, while the resonance frequency ω_i is related to the bandwidth of the WF model. The 6×1 disturbance matrix is written:

$$\Gamma_W = [k_1, \ k_2, \ k_3, \ 0, \ 0, \ 0]^T \qquad (23)$$

where k_1 , k_2 and $k_3 > 0$ are the covariance of the white noise process reflecting the WF response caused by the actual sea state. k_1 , k_2 and k_3 are linearly dependent on the significant wave height. The 3×6 measurement matrix is written:

$$C_W = [I_{3\times3} \quad 0_{3\times3}]. \qquad (24)$$

The sensor noise in the WF model is omitted, since it has already been modelled in the LF model.

2.3 Linear Thruster Model

Usually, perfect control action without imposing the thruster dynamics are assumed. Unfortunately, this will not be true in a real system. The thrust response is affected by the dynamics in the actuators and the drive system. This will cause reduced command- following capabilities such as phase lag and amplitude reduction when the frequency increases. There will also be a loss of thrust efficiency due to disturbances in the water inflow to the thruster blades, caused by thrust-to-thrust and thrust-to-hull interactions, current and vessel velocities. In addition the influence from the free surface will affect the thrust efficiency. Reduced thruster efficiency caused by disturbances in the water inflow is compensated for in the thrust allocation algorithm. The dynamics in the actuator and drive systems will be accounted for in the controller. Experience obtained from full-scale experiments indicates that a first-order model is well suited to this purpose. Hence, the thruster dynamics is represented by the following model:

$$\dot{\tau} = -A_{tr}\tau + A_{tr}\tau_c \qquad (25)$$

where τ_c is the commanded thrust forces and moment vector. The 3×3 diagonal thruster dynamics matrix is defined as:

$$A_{tr} = \text{diag}\left(\frac{1}{T_{tr1}}, \quad \frac{1}{T_{tr2}}, \quad \frac{1}{T_{tr3}}\right). \qquad (26)$$

Here, T_{tr1}, T_{tr2} and T_{tr3} are the equivalent thruster time constants in surge, sway and yaw. For a conventional thruster system T_{tr1} can be approximated by the time constants corresponding to the main propellers. T_{tr2} and T_{tr3} can be approximated by the time constants to the tunnel and azimuth thrusters. Moreover, it is reasonable to assume that $T_{tr2} \approx T_{tr3}$.

3. DP CONTROLLER DESIGN

The DP controller consists of a feedback controller and a feedforward controller. The proposed feedback control loop was inspired by the work of Balchen (1993) and is modified for the purpose of DP application. The computation of feedback signals to be used in the controller are based on Kalman filter and observer theory.

3.1 Control Design Plant Model

In order to produce the desired control action, a design plant model to be used in conjunction with the controller is derived according to:

$$\dot{\hat{x}} = A\hat{x} + B\tau_c \qquad (27)$$

where the 9-dimensional estimated state-space vector is defined as $\hat{x} = \left[\hat{x}_L^T, \quad \hat{\tau}^T\right]^T$. The 9×9 augmented system matrix is written:

$$A = \begin{bmatrix} A_L & B_L \\ 0_{3\times3} & -A_{tr} \end{bmatrix}. \qquad (28)$$

The 9×3 control input matrix B becomes:

$$B = \begin{bmatrix} 0_{6\times3} \\ A_{tr} \end{bmatrix}. \qquad (29)$$

3.2 Reference Model

For DP operations close to other offshore structures or ships, it is crucial to be capable to perform controlled movements and rotations of the vessel. The automatic guidance function which takes the vessel from the prevailing setpoint coordinates to the new setpoint is defined as the "marked position", and can be specified either in the vessel-parallel frame or in the earth-fixed frame. The movement and rotation can be done for each degree of freedom separately, or as a fully 3 DOF coupled motion. In order to provide high-performance DP operations with bumbles transfer between station-keeping and marked position operations, a reference model is introduced for the calculation of feasible trajectories of the desired vessel motion for each degree of freedom. Experience achieved from full-scale experiments has demonstrated that the following reference model in the earth-fixed frame is appropriate (Fossen, 1994):

$$a_d^e + \Omega v_d^e + \Gamma x_d^e = \Gamma x_{ref}^e . \qquad (30)$$

The 3-dimensional vectors a_d^e, v_d^e and x_d^e define the desired vessel acceleration, velocity and position trajectories in the earth-fixed frame. The vector x_{ref}^e defines the new reference coordinates, either relative to the previous setpoint, or as global earth-fixed coordinates. The design parameters in the reference model consist of a 3×3 diagonal damping matrix $\Omega > 0$ and a 3×3 diagonal stiffness matrix $\Gamma > 0$. The earth-fixed desired vessel acceleration, velocity and position trajectories are transformed into a moving vessel-parallel frame which follows the desired earth-fixed position and heading trajectory. Hence:

$$a_d = J^T a_d^e, \; v_d = J^T v_d^e, \; x_d = J^T x_d^e . \qquad (31)$$

The reference model will also run in station-keeping operations, but then with the desired velocity and acceleration equal to zero. This provides a smooth transfer between the two operational modes.

3.3 LQG Control Law

The proposed LQG algorithm takes the deviation vector between the state estimate vector and the desired state vector and produces a proportional feedback to the control vector. Assuming that the nominal vessel and thruster model is detectable and stabilisable, the LQG feedback control law is derived by minimising the following performance index:

$$J = E\left\{\lim_{T\to\infty} \frac{1}{T}\int_0^T \left(e^T Q e + \tau_{LQ}^T P \tau_{LQ}\right) dt\right\}. \qquad (32)$$

The deviation vector is defined as:

$$e = \left[e_1^T, \quad e_2^T, \quad e_3^T\right]^T \qquad (33)$$

where

$$e_1 = \left[\hat{u}, \quad \hat{v}, \quad \hat{r}\right]^T$$
$$e_2 = \left[\hat{x}, \quad \hat{y}, \quad \hat{\psi}\right]^T$$
$$e_3 = \hat{\tau} - \tau_{FF} - \tau_I - \tau_d \, .$$

Here, $\hat{\tau}$ is the estimated thruster forces and moment vector in surge, sway and yaw. $Q = Q^T \geq 0$ is a 9× 9 error weighting matrix and $P = P^T > 0$ is a 3×3 control weighting matrix. By minimising the control index J, the LQG method returns the control gain matrix G_{LQ}. For linear time-invariant systems, stationary solutions of the Ricatti equation can be found. Hence, the Ricatti equation computations reduce to solving:

$$-AR_\infty - A^T R_\infty + R_\infty B P^{-1} B^T R_\infty - Q = 0 \quad (34)$$

where R_∞ is a 9×9 non-negative symmetric matrix. The 3×9 stationary LQG control gain matrix is:

$$G_{LQ} = P^{-1} B^T R_\infty \, . \quad (35)$$

The LQG control law is then:

$$\tau_{LQ} = -G_{LQ} e \, . \quad (36)$$

3.4 Integral Action

In order to meet the special command-following and disturbance-rejection performance specifications, it is necessary to append three free integrators to the control model. It is then desirable to define a property space z which expresses the variables to be controlled towards certain setpoints (Balchen, 1993). The dimension of the property space is the same as the control vector space, that is $\tau \in \Re^3$ implies that $z \in \Re^3$. The variables to be controlled to the setpoints are fewer than those constituting the state space $e \in \Re^9$. The relation between these variables and the state space is given through the transformation:

$$z = g(e) = e_2 \, . \quad (37)$$

A multivariable PI algorithm is then achieved by means of an integral loop, controlling the property z in parallel with the proportional LQ control loop. Inspired by classical SISO PI controller tuning, one can specify the eigenvalues of the integral loop in a diagonal matrix Λ_G . Since the integral loop will be slower than the proportional LQ loop, the following approximation for the integral loop can be found:

$$\dot{z} = G_I G_z \left(A - B G_{LQ}\right)^{-1} B \, z = \Lambda_G z \quad (38)$$

where G_z is a 3×9 property matrix given by:

$$G_z = \frac{\partial g(e)}{\partial e} = \left[0_{3\times3} \quad I_{3\times3} \quad 0_{3\times3}\right] . \quad (39)$$

This leads to the 3×3 integral loop-gain matrix:

$$G_I = \Lambda_G \left(G_z \left(A - B G_{LQ}\right)^{-1} B \right)^{-1} \quad (40)$$

where the matrix $G_z(A\text{-}BG_{LQ})^{-1}B$ must be non-singular. Open integrators, as they appear both in the control loop and the estimator, are equipped with anti-windup precautions in case their outputs reach amplitude restrictions such as saturation in the physical control devices. The resulting integral control law is written:

$$\dot{\tau}_I = A_{WI} \tau_I + G_I \, z \quad (41)$$

where A_{WI} is a 3×3 anti-windup precaution matrix.

3.5 Wind Feedforward Controller

Wind loads have an important impact on the vessel's response. In order to obtain fast disturbance rejection with respect to varying wind loads, it is desirable to introduce a wind feedforward controller. The wind forces and moment in surge, sway and yaw are estimated by a Kalman filter and a Luenberger observer, where the wind velocity and wind direction are measured. The estimates are multiplied by a feedforward gain matrix. The wind feedforward control law is taken to be:

$$\tau_{FF} = -G_W \hat{\tau}_{wind} \quad (42)$$

where $\hat{\tau}_{wind}$ is the estimated wind forces and moment in surge, sway and yaw respectively. It is assumed that the wind loads are uncoupled, such that the gain matrix G_W is a 3×3 diagonal matrix:

$$G_w = \mathrm{diag}\left(g_{w1}, \quad g_{w2}, \quad g_{w3}\right) \quad (43)$$

where $0 \leq g_{wi} \leq 1$ for i = 1,..,3.

3.6 Model Reference Feedforward Controller

In order to improve the performance of the controller during marked position (tracking) operations a feedforward control action based on input from the reference model is included. The feedforward control action is derived to be:

$$\tau_d = Ma_d + D_L v_d + C_{RB}(v_d)v_d + C_A(v_d)v_d \quad (44)$$

3.7 Resulting DP Control Law

The resulting DP control law is found by adding (36), (41), (42) and (44), that is:

$$\tau_c = \tau_{LQ} + \tau_I + \tau_{FF} + \tau_d . \quad (45)$$

3.8 Optimal Thrust Allocation

The relation between the equivalent control vector τ_c and the actual thruster action u_c is defined according to:

$$\tau_c = TKu_c \quad (46)$$

where T is a 3×r thrust configuration matrix and r is the number of thrusters. K is a r×r diagonal matrix of thrust force coefficients (Fossen *et al.*, 1995) and u_c is the actual control vector of either pitch-controlled or revolution-controlled propeller inputs. If the number of control inputs r is not equal to the number of outputs (surge, sway and yaw) to be controlled, the thrust configuration matrix becomes singular and the inverse matrix cannot be found. Then the inverse thrust configuration matrix T^{-1} is replaced with the generalised inverse T^{+}. This matrix may be found by minimising the quadratic energy cost function according to:

$$\min J = \frac{1}{2}(Ku_c)^T W(Ku_c), \quad (47)$$

subject to:

$$\tau_c - TKu_c = 0, \quad (48)$$

where W is a r×r positive definite matrix providing mutual weighting of the different thrusters with respect to minimum control energy. W is usually diagonal, and the diagonal elements should be selected such that the control actions are directed towards the desired thruster. The large element in W means that the actual thruster is expensive to use. The solution of the optimisation problem is written:

$$T^{+} = W^{-1}T^T\left(TW^{-1}T^T\right)^{-1}. \quad (49)$$

Hence, the commanded control action provided by the actual thrusters becomes:

$$u_c = K^{-1}T^{+}\tau_c . \quad (50)$$

4. FULL-SCALE RESULTS

A dynamic positioning (DP) system has been implemented by using ABB Master and Advant products. Experience obtained from commercial installations of the ABB DP system has successfully demonstrated the performance of the proposed controller. In this paper results from full-scale experiments with the multipurpose supply ship, Northern Clipper, operating at oil and gas fields in the North Sea are shown. The installed ABB DP system configuration and Northern Clipper are illustrated in Figs. 2 and 3.

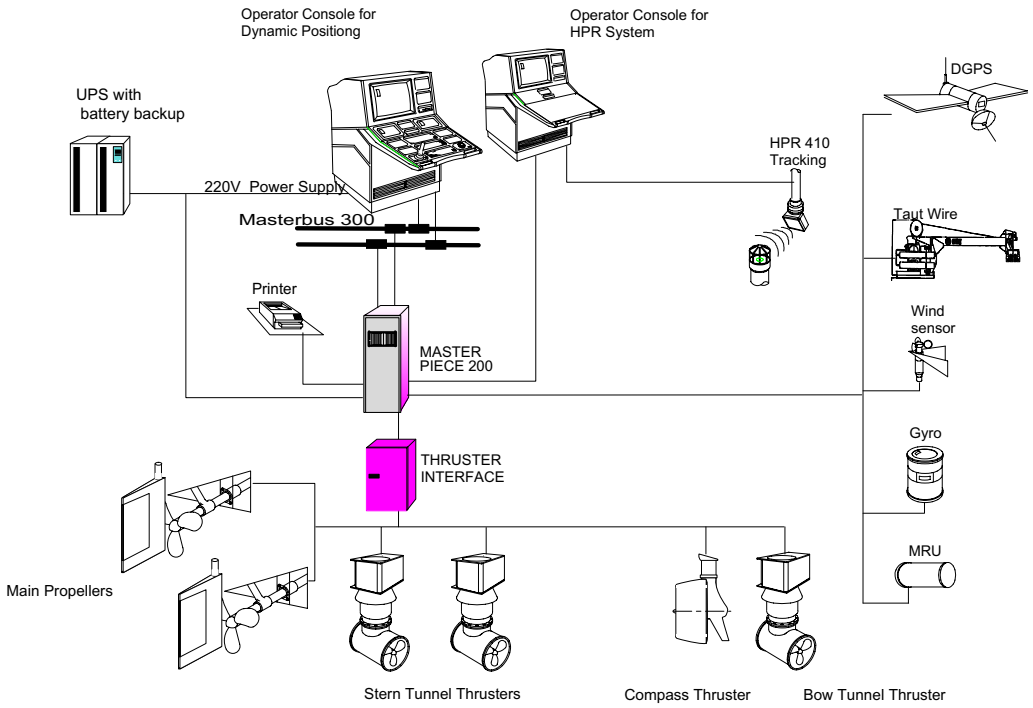

Fig. 2. The ABB DP system configuration for Northern Clipper.

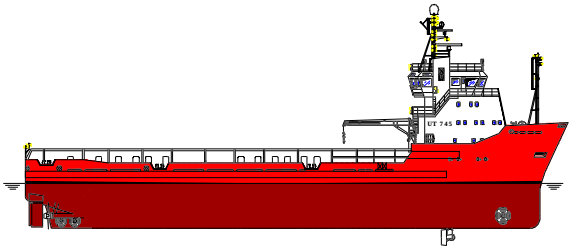

Fig. 3. Northern Clipper owned by Sævik Supply Management.

The main dimensions of the vessel are: design draught is 6.25 m, vessel dead-weight at draught 6.25 m is 4200 ton, length between the perpendiculars is 82.5 m. Northern Clipper is equipped with two main propellers, two stern tunnel thrusters, one bow tunnel thruster and one compass thruster. The main engine consists of two 3530 kW Ulstein Bergen engines. Three different types of position reference systems are installed; a differential GPS, a taut wire and an underwater based hydroacoustic position reference (HPR) system.

In Figs. 4-8 time series recorded on Northern Clipper are shown. All the time series were recorded during the same DP operation. The vessel was operated in station-keeping function for 60 s. Then the operator changed the setpoint and commanded the vessel to move 18 m to the south and 19 m to the east without changing the heading. After about 300 s the vessel reached the new desired position, and then the DP system automatically returned to station-keeping function. The significant wave height was about 1 m and the mean wind velocity was 10 m/s, with zero relative direction.

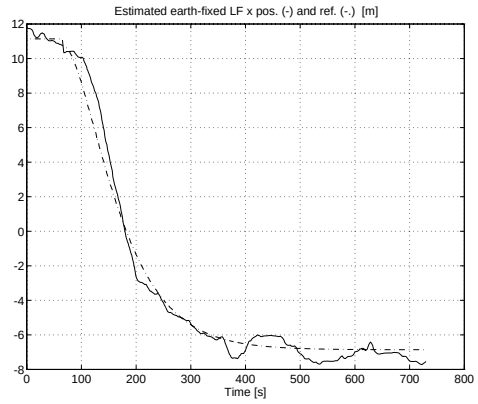

Fig. 4. Estimated (-) and desired (-·) earth-fixed x position during station-keeping and marked position operations with Δx=-18 m, Δy=19 m and $\Delta\psi$ = 0 deg.

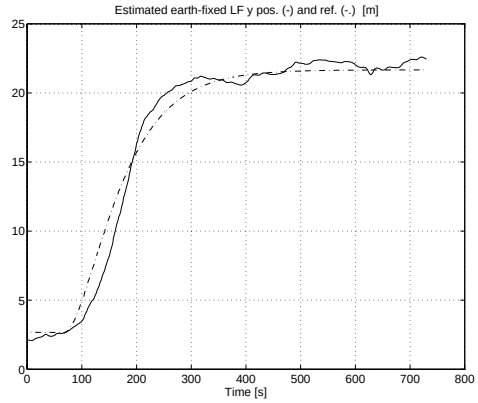

Fig. 5. Estimated (-) and desired (-·) earth-fixed y position during station-keeping and marked position operations with Δx=-18 m, Δy=19 m and Δψ = 0 deg.

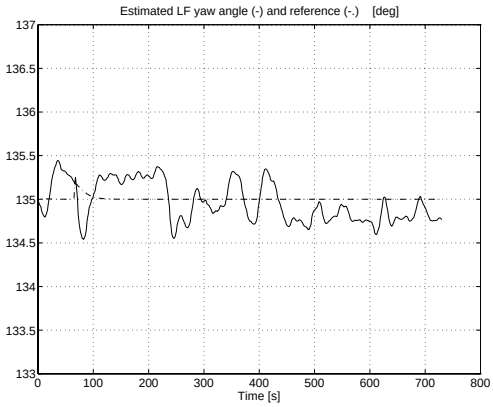

Fig. 6. Estimated (-) and desired (-·) heading angle ψ angle during station-keeping and marked position operations with Δx=-18 m, Δy=19 m and Δψ = 0 deg.

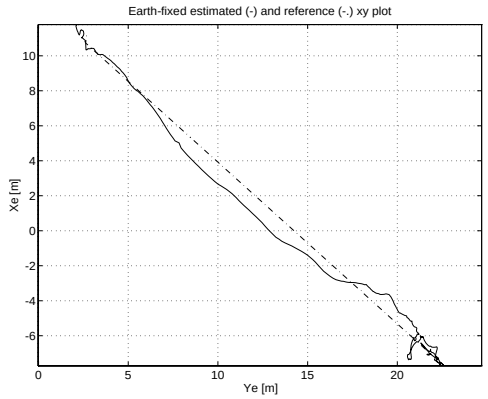

Fig. 7. Estimated (-) and desired (-·) xy-plot of marked position and station-keeping operations with Δx=-18 m, Δy=19 m and Δψ= 0 deg.

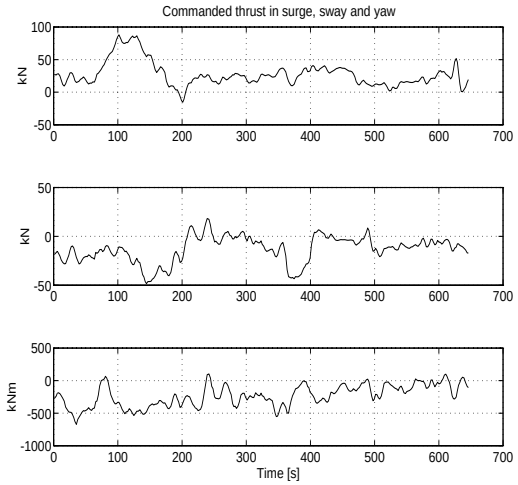

Fig. 8. Commanded thrust during station-keeping and marked position operations.

5. CONCLUSIONS

A dynamic positioning (DP) system using model-based control has been proposed. Commercial DP systems have different control modes for automatic positioning and guidance of marine vessels by means of thruster and propeller actions. This paper describes a control scheme which provides bumbles transfer between station-keeping and tracking (marked position) operations. A reference model is used to provide appropriate reference trajectories. Since it is not desirable to counteract the wave-frequency movement caused by first-order wave loads, the control actions of the propulsion system are produced by the low-frequency part of the vessel movement, caused by current, wind and second-order mean and slowly varying wave loads. Kalman filter theory is used for state estimation. Full-scale experiments with a multipurpose supply ship have successfully demonstrated the performance of the proposed controller.

ACKNOWLEDGEMENTS - ABB Industri AS, ABB Corporate Research Norway, Sævik Supply Management AS and Norsk Hydro AS are gratefully acknowledged for fruitful cooperation and contributions.

6. REFERENCES

Balchen, J. G. (1993). A Modified LQG Algorithm (MLQG) for Robust Control of Nonlinear Multivariable Systems. *Modeling, Identification and Control*, Vol. (**14)**, No. (3), pp. 175-180.

Balchen, J. G., N. A. Jenssen and S. Sælid (1976). Dynamic Positioning Using Kalman Filtering and Optimal Control Theory. *IFAC/IFIP Symp. on Aut. in Offshore Oil Field Operation*, Holland, Amsterdam, pp. 183-186.

Balchen, J. G., N. A. Jenssen and S. Sælid (1980a). Dynamic Positioning of Floating Vessels Based on Kalman Filtering and Optimal Control. *Proc. of the 19th IEEE Conf. on Decision and Control*, Albuquerque, N.M., pp. 852-864.

Balchen, J. G., N. A. Jenssen, E. Mathisen and S. Sælid (1980b). A Dynamic Positioning System Based on Kalman Filtering and Optimal Control. *Modeling, Identification and Control*, Vol. (**1**), No. (3), pp. 135-163.

Faltinsen, O. M., L. Dahle and B. Sortland (1986). Slowdrift Damping and Response of a Moored Ship in Irregular Waves. *Proc. 3rd OMAE Conf.*, Tokyo, Japan.

Faltinsen, O. M. and B. Sortland (1987). Slow Drift Eddy Making Damping of a Ship. *Applied Ocean Research*, Vol. **9**, No. 1, pp. 37-46.

Faltinsen, O. M. (1990). *Sea Loads on Ships and Offshore Structures*. Cambridge University Press.

Fossen, T. I. (1994). *Guidance and Control of Ocean Vehicles*. John Wiley and Sons Ltd.

Fossen, T. I., S. I. Sagatun and A. J. Sørensen (1995). Identification of Dynamically Positioned Ships. *Proc. of the 3rd IFAC Workshop on Control Applications in Marine Systems* (CAMS'95), Trondheim, Norway, pp. 362-369.

Fung, P. T-K. and M. Grimble (1983). Dynamic Ship Positioning Using Self-Tuning Kalman Filter. *IEEE Trans. on Aut. Con.* **AC-28** (3), pp. 339-349.

Grimble, M. J., R. J. Patton and D. A. Wise (1980a). The Design of Dynamic Ship Positioning Control Systems Using Stochastic Optimal Control Theory. *Opt. Con. Appl. and Meth.*, **1**, pp. 167-202.

Grimble, M. J., R. J. Patton and D. A. Wise (1980b) Use of Kalman Filtering Techniques in Dynamic Ship Positioning Systems. *IEE Proc.*, Vol. **127**, No. 3, Pt. D, pp. 93-102.

Isherwood, M. A. (1972). Wind Resistance of Merchant Ships. *Trans. Inst. Naval Arch.*, RINA, Vol. **115**, pp. 327-338.

Newman, J. N. (1974). Second Order Slowly Varying Forces on Vessels in Irregular Waves. *Proc. Int. Symp. on the Dyn. of Mar. Vehicles and Struct. in Waves*, London, England, pp. 182-186.

Newman, J. N. (1977). *Marine Hydrodynamics.* MIT Press, Cambridge, Massachusetts.

Sælid, S., N. A. Jenssen and J. G. Balchen (1983). Design and Analysis of a Dynamic Positioning System Based on Kalman Filtering and Optimal Control. *IEEE Trans. on Aut. Con.* **AC-28** (3), pp. 331-339.

Wichers, J.E.W. (1993). Position Control - From Anchoring to DP system. *UETP, Marine Science and Technology*, Trondheim, Norway, Section 18, pp. 1-23.